AGU PUBLICATIONS

Geophysical Research Letters

RESEARCH LETTER
10.1002/2017GL074216

Key Points:
- Much of the central and western Ross Sea deglaciated abruptly ~9-8 kyr B.P.
- The Ross Sea Sector did not significantly contribute or respond to MWP-1A
- Rapid deglaciation was likely influenced by retreat into marine basins and/or enhanced marine melting

Supporting Information:
- Supporting Information S1
- Table S1

Correspondence to:
P. Spector,
pspec@uw.edu

Citation:
Spector, P., J. Stone, S. G. Cowdery, B. Hall, H. Conway, and G. Bromley (2017), Rapid early-Holocene deglaciation in the Ross Sea, Antarctica, *Geophys. Res. Lett.*, *44*, 7817–7825, doi:10.1002/2017GL074216.

Received 19 MAY 2017
Accepted 18 JUL 2017
Accepted article online 25 JUL 2017
Published online 12 AUG 2017
Corrected 28 AUG 2017

This article was corrected on 28 AUG 2017. See the end of the full text for details.

Rapid early-Holocene deglaciation in the Ross Sea, Antarctica

Perry Spector[1], John Stone[1], Seth G. Cowdery[1], Brenda Hall[2], Howard Conway[1], and Gordon Bromley[2]

[1]Department of Earth and Space Sciences, University of Washington, Seattle, Washington, USA, [2]School of Earth and Climate Sciences and Climate Change Institute, University of Maine, Orono, Maine, USA

Abstract Deglaciation of the Ross Sea following the last ice age provides an important opportunity to examine the stability of marine ice sheets and their susceptibility to changing environmental conditions. Insufficient chronology for Ross Sea deglaciation has helped sustain (i) the theory that this region contributed significantly to Meltwater Pulse 1A (MWP-1A) and (ii) the idea that Ross Sea grounding-line retreat occurred in a "swinging gate" pattern hinged north of Roosevelt Island. We present deglaciation records from southern Transantarctic Mountain glaciers, which delivered ice to the central Ross Sea. Abrupt thinning of these glaciers 9–8 kyr B.P. coincided with deglaciation of the Scott Coast, ~800 km to the north, and ended with the Ross Sea grounding line near Shackleton Glacier. This deglaciation removed grounded ice from most of the central and western Ross Sea in less than 2 kyr. The Ross Sea Sector neither contributed nor responded significantly to MWP-1A.

1. Introduction

The West Antarctic Ice Sheet (WAIS) is regarded as vulnerable to unstable retreat because much of it rests below sea level on a bed that deepens inland [*Weertman*, 1974; *Schoof*, 2007]. The ice sheet likely collapsed during at least one Pleistocene interglacial period [*Scherer et al.*, 1998], and an incipient collapse may be underway in the Amundsen Sector [*Joughin et al.*, 2014; *Rignot et al.*, 2014]. This potential instability emphasizes the importance of understanding how marine ice sheets receded in the past. The Antarctic Ice Sheet has been identified as a significant source of Meltwater Pulse 1A (MWP-1A), [e.g. *Clark et al.*, 2002], an abrupt ~9–20 m eustatic sea-level rise 14.6 kyr before present (BP) [*Liu et al.*, 2016; *Lambeck et al.*, 2014; *Deschamps et al.*, 2012; *Peltier et al.*, 2015]. Attention has turned to the large Ross and Weddell marine embayments as possible Antarctic source areas; however, most geological and glaciological studies argue against a large Antarctic contribution from either sector [*The RAISED Consortium et al.*, 2014, and references therein]. In the case of the Ross Sea, most chronological constraints come from the seafloor north of the Ross Ice Shelf and deposits along the NW coast (Figure 1), leaving the deglacial history of the southern Ross Embayment largely unknown.

An enduring paradigm of Ross Sea deglaciation is the "swinging gate" model, in which the grounding line retreated along the Transantarctic Mountains while hinged north of Roosevelt Island (Figure 1) until ~3 kyr B.P. [*Stuiver et al.*, 1981; *Conway et al.*, 1999; *Martín et al.*, 2006]. This depiction arose primarily from constraints in the western Ross Embayment north of Hatherton Glacier (Figure 1). Detailed seafloor mapping has since revealed geomorphic evidence for a complex recession north of the modern ice shelf, in which periods of grounding-line stability were interrupted by episodes of rapid retreat [*Anderson et al.*, 2014; *Halberstadt et al.*, 2016]. Although attempts to date the retreat in the central and eastern Ross Sea have been inconclusive [*Anderson et al.*, 2014], retreat ages in the western Ross Sea show that final deglaciation of the Scott Coast region occurred ~8.6–7 kyr B.P. (see section 4.3).

Here we present deglaciation records based on ^{10}Be exposure ages of glacial deposits for Beardmore, Shackleton, and Scott Glaciers in the southern Transantarctic Mountains (Figure 1). We show that the grounding line had reached the mouths of Beardmore and Shackleton Glaciers by ~8 kyr B.P. (Figure 1). Combined with previously published constraints from the Scott Coast region, the data demonstrate that most of the central and western Ross Sea became ice free in an episode of rapid grounding-line retreat in the early Holocene.

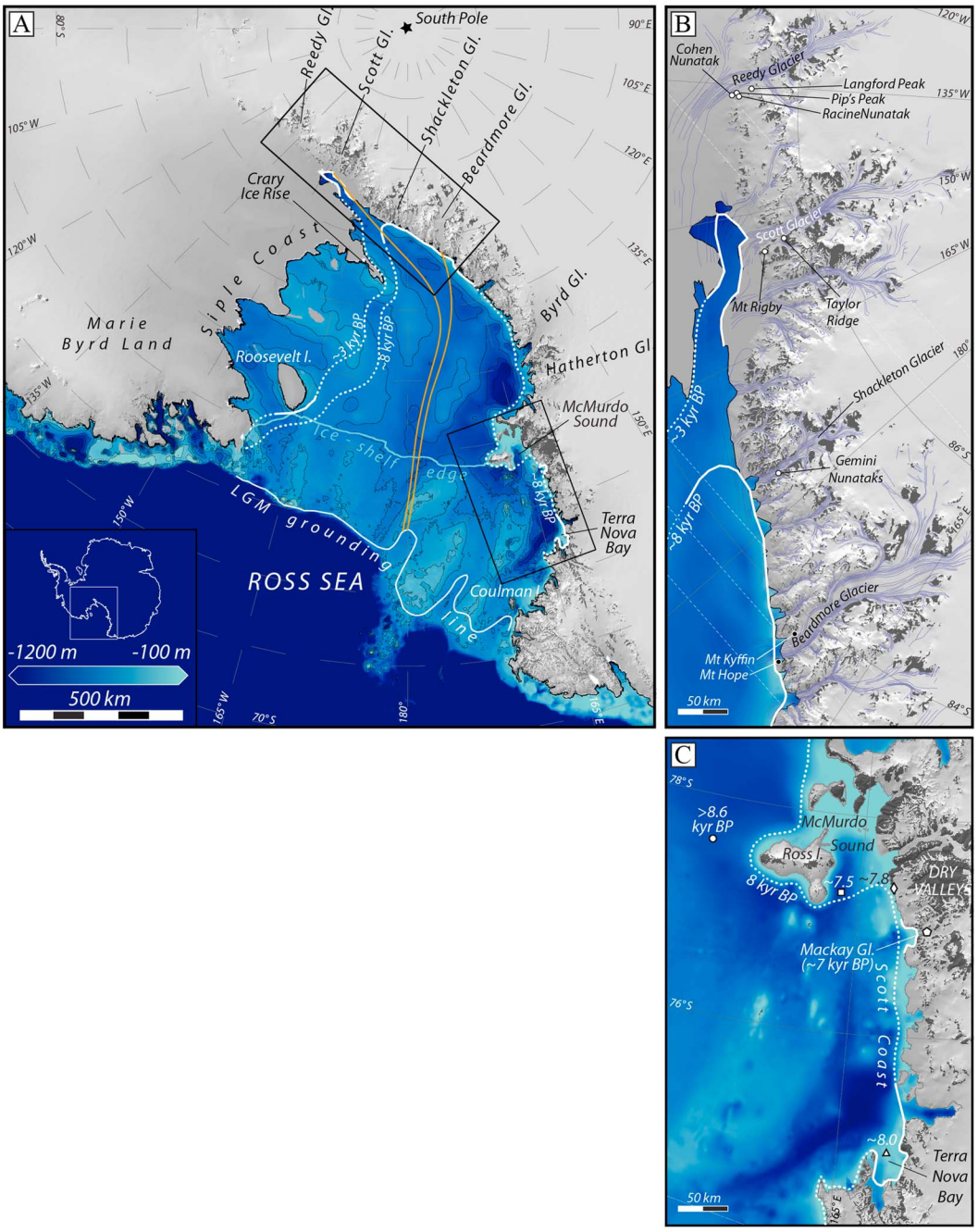

Figure 1. (a) The Ross Sector of Antarctica, showing rock and ice surfaces [*Liu et al.*, 2001] and marine bathymetry [*Fretwell et al.*, 2013]. Black rectangles show the locations of (b) a map of the southern Transantarctic Mountains and our field sites and (c) a map of the Scott Coast region. Orange lines represent inferred locations of flowlines from Scott and Beardmore Glaciers. These flowlines are schematic and are drawn to obey the provenance of till near the LGM grounding line [*Licht et al.*, 2014]. The LGM grounding line is from *Halberstadt et al.* [2016]. In Figures 1a–1c, white contours (solid where constrained by observations; dotted where inferred) represent the grounding-line chronology based on results presented here from the southern Transantarctic Mountains, from Roosevelt Island [*Conway et al.*, 1999; *Martín et al.*, 2006], and from the Scott Coast region. Because Crary Ice Rise is thought to have regrounded ~1.1 kyr B.P. [*Bindschadler et al.*, 1990], the grounding line may have been inboard of this location during the late Holocene. In the Scott Coast region (Figure 1c), the timing of final deglaciation is constrained by the following studies: *Baroni and Hall* [2004] (diamond), *Hall et al.* [2004] (triangle), *Jones et al.* [2015] (pentagon), *Licht et al.* [1996] (square), and *McKay et al.* [2016] (circle).

2. Field Sites and Methods

Beardmore, Shackleton, and Scott Glaciers flow through the southern Transantarctic Mountains and deliver ice to the central Ross Sea. Provenance studies indicate a similar flow pattern during the last ice age [*Anderson et al.*, 2014; *Licht et al.*, 2005, 2014; *Farmer et al.*, 2006]. These glaciers transported rocks quarried upstream to ablation zones along their margins in the Transantarctic Mountains, depositing small lateral moraines and thin debris sheets during the glacial maximum and scattered erratics during deglaciation (Figures S1–S9 in the supporting information).

We sampled deposits on Taylor Ridge and Mount Kyffin (Figures 1b, S3, and S9) that mark the maximum ice age thickness of the lower reaches of Scott and Beardmore Glaciers, respectively. At the mouths of these glaciers, Mount Rigby and Mount Hope were both overrun during the glacial maximum but their summits emerged early in the deglaciation. We collected elevation transects of lightly weathered glacial erratics on these mountains to chronicle Ross Sea deglaciation at the mouths of Scott and Beardmore Glaciers (Figures S1 and S6). We found no fresh glacial deposits on mountains at the mouth of Shackleton Glacier, but we sampled a short elevation transect of fresh erratics from Gemini Nunataks, a pair of small peaks ~25 km upstream from the glacier mouth (Figure S5). The low relief of this site (~50 m) only constrains the final thinning of Shackleton Glacier.

For rock freshly eroded from the glacier bed, transported to the surface, and stranded by thinning ice, the subsequent buildup of cosmic ray-produced ^{10}Be records the time since initial exposure in the ablation zone. Details of the exposure-dating technique are described in the supporting information [*Balco et al.*, 2008; *Borchers et al.*, 2016; *Briggs et al.*, 2014; *Ditchburn and Whitehead*, 1994; *Jull et al.*, 2015; *Kohl and Nishiizumi*, 1992; *Lal*, 1991; *Nishiizumi et al.*, 2007; *Stone*, 2000]. Localized ablation zones are found on Antarctic glaciers, commonly in areas exposed to descending and warming katabatic winds. Ablation in these areas brings englacial debris to the glacier surface and ultimately results in deposition. During times when the glacier surfaces were stable or changing slowly, such as the Last Glacial Maximum (LGM), cobbles may have been exposed hundreds or thousands of years before physical deposition on bedrock [*Ackert Jr. et al.*, 2011]. In this case, exposure ages from a deposit are likely to span the period of stable ice thickness rather than date their final deposition. At times of rapid thinning, predepositional exposure is unlikely to be more than a few hundred years, less than the uncertainty of the exposure age.

Potential exposure-dating complications in Antarctica include shielding by snow cover, postdepositional disturbance by periglacial processes, and recycling of rock from older deposits. To avoid disturbance and snow cover, we sampled isolated erratics resting directly on windswept bedrock surfaces or on the surface of older, consolidated glacial deposits. To minimize the effect of recycling and prior exposure, we sampled only fresh, glacially worked erratics. Nonetheless, our samples include several rocks with substantially older exposure ages than other rocks collected nearby (Figure 2). In such cases, because we can eliminate the possibility of postdepositional erosion, disturbance, and cover by snow or till, we interpret the younger age as dating deposition and the older apparent age as the result of prior exposure. With allowance for these few cases of prior exposure and recycling, transects at all three sites show monotonically decreasing exposure ages with decreasing altitude (Figure 2).

Beryllium-10 production rates by spallation are based on the global calibration data set by *Borchers et al.* [2016], adjusted for altitude and latitude using the scaling scheme by *Lal* [1991] and the relationship between Antarctic air pressure and elevation [*Stone*, 2000]. Some recent production rate calibrations suggest lower values than that of *Borchers et al.* [2016]. Using other combinations of high-latitude calibration data sets and scaling schemes would increase exposure ages by 1–6%, which would not substantially affect the findings of this research.

3. Results

3.1. Glacial Maximum in the Southern Ross Sea

At Taylor Ridge, 20 km upstream from the mouth of Scott Glacier, a lateral moraine at 1200 m marks the maximum elevation of ice during the LGM. The depositional limit consists of scattered boulders and perched cobbles resting stably on an older, heavily weathered glacial deposit (Figure S9). Apparent exposure ages of the LGM deposits range from 19.4 ± 0.6 to 16.4 ± 0.3 kyr B.P. (Figure 2b). At Mount Kyffin, ~10 km upstream from the mouth of Beardmore Glacier, the upper limit of an ablation till at ~1050 m marks the maximum

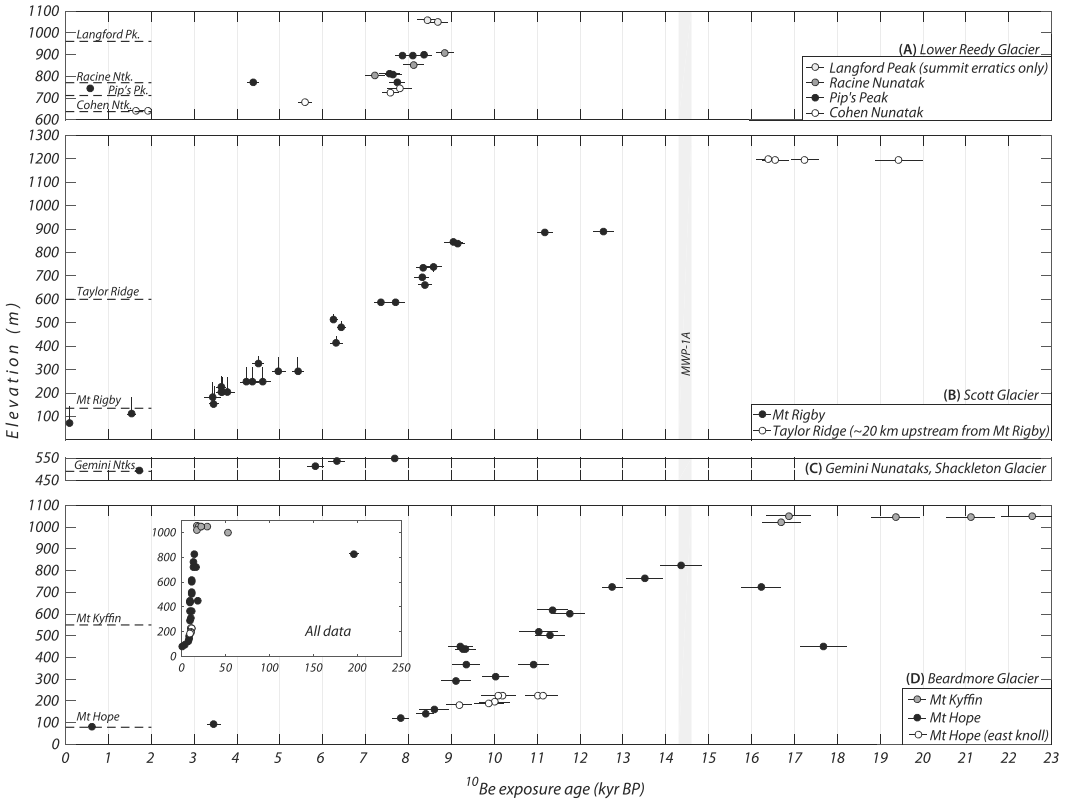

Figure 2. Exposure ages of glacial deposits, plotted versus elevation. See Figure 1 for site locations. (a) Lower Reedy Glacier nunataks [*Todd et al.*, 2010]. (b) Mount Rigby and Taylor Ridge at Scott Glacier. (c) Gemini Nunataks at Shackleton Glacier. (d) Mount Hope and Mount Kyffin at Beardmore Glacier. Inset shows the apparent exposure ages of all samples from these sites. For Figures 2a–2d, the modern glacier surface elevations are represented by horizontal dashed lines, and the gray vertical bar represents the timing of MWP-1A [*Carlson and Clark*, 2012]. See supporting information for discussion of sample elevations in Figures 2b–2d.

elevation of LGM glacier ice. The deposit is ice-cored in places and consists of relatively unweathered cobbles and boulders overlying older glacial deposits and felsenmeer surfaces (Figures S3 and S4). Here we primarily sampled boulders resting on other much larger, stable, boulders. Exposure ages range from 52.3 ± 1.4 to 16.7 ± 0.5 kyr B.P. (Figure 2d). The two oldest ages are artifacts of prior exposure; the spread of the remaining ages from 22.5 to 16.7 kyr B.P. may represent a prolonged glacial maximum or lesser degrees of prior exposure. In either case, these highstands were sustained at both sites until ~17–16 kyr B.P. and possibly later, given that we may not have collected the youngest rocks at each site.

During the LGM, Scott Glacier ice descending from 1200 m at Taylor Ridge must have covered Mount Rigby (893 m), located at the glacier mouth (Figure 1b) by significantly less than 300 m. Mount Rigby remained ice-covered until 12.5 ± 0.3 kyr B.P. (Figure 2b). Minimal thinning occurred between the onset of deglaciation at Taylor Ridge and the emergence of Mount Rigby's summit, spanning the period of MWP-1A. Across the mouth of Beardmore Glacier from Mount Kyffin, Mount Hope (836 m) remained ice covered until 14.4 ± 0.5 kyr B.P. (Figure 2d). No more than ~200 m of thinning, and potentially much less, could have occurred at Beardmore Glacier during the MWP-1A interval.

3.2. Rapid Thinning of Southern Ross Sea Glaciers

3.2.1. Scott Glacier

Below the summit of Mount Rigby, exposure ages decrease with elevation and record rapid thinning of Scott Glacier at ~8.4 and ~6.3 kyr B.P. (Figure 2b). After the second of these events, the ice surface gradually lowered over the next ~3 kyr to near the modern glacier level. The two lowest and youngest samples from Mount Rigby come from an ablation hollow in the surrounding, near-stagnant debris field, below modern glacier level (Figure S6). This area northeast of Mount Rigby apparently stagnated between ~3.5 and ~1.5 kyr B.P.

(Figure 2b) and has since ablated by tens of meters; exposure of these two samples was not connected to further lowering of the glacier surface.

3.2.2. Beardmore Glacier

Erratics from Mount Hope's southeast ridge record gradual thinning of the margin of Beardmore Glacier to an elevation of 440 m by ~9.3 kyr B.P. (Figure 2d). The ice surface then abruptly dropped ~280 m over the next 700 ± 200 years to within 80 m of the modern glacier level. Five samples from the Mount Hope transect are clearly older than samples collected nearby at similar elevations, and these older ages are interpreted to be the result of prior exposure. We also collected erratics from a small knoll on the east side of Mount Hope (Figure S1). Ages there are consistently 1–2 kyr older than the elevation transect described above (Figure 2d). It appears that this part of the mountain was exposed earlier than the southeast ridge. This may have resulted from higher ablation (due to its northerly aspect or wind circulation around the peak) or from the propensity for ice to flow past the sharp southeast ridge rather than divert into the lee of the ridge. The same effects keep the modern Ross Ice Shelf surface ~80 m lower north of the peak than below the southeast ridge.

3.2.3. Shackleton Glacier

At Shackleton Glacier, our deglaciation record only extends ~50 m above the modern ice (Figures 2c and S5), but it reveals that the highest point on Gemini Nunataks became exposed 7.7 ± 0.2 kyr B.P., indicating near-complete deglaciation of lower Shackleton Glacier by this time (Figure 2c).

3.2.4. Reedy Glacier

Small nunataks at the mouth of Reedy Glacier (Langford Peak, Racine Nunatak, Cohen Nunatak, and Pip's Peak), which are ~130 km upstream of the modern Siple Coast grounding line (Figure 1b), record the last stages of ice thinning farther along the Transantarctic Mountains. Data from *Todd et al.* [2010], which have been recalculated to be consistent with samples presented in this paper, show that the summits of these nunataks became ice free ~8.8–7.8 kyr B.P., and except for Cohen Nunatak, their lower slopes were exposed within the following few thousand years, establishing the modern ice surface at these sites (Figure 2a). Deglaciation of these peaks overlapped with rapid ice thinning at Mount Hope and Mount Rigby.

4. Discussion

4.1. Relation Between Grounding-Line Retreat and Upstream Thinning

Deglaciation at the mouths of four major outlet glaciers described in section 3 was largely confined to the early Holocene and included abrupt events that removed hundreds of meters of ice in periods on the order of ~1 kyr. The thinning records provide information about grounding-line retreat in the Ross Sea, discussed below in section 4.2. Establishment of present-day ice levels on lower Beadmore, Shackleton, and Scott Glaciers (Figure 2) requires the grounding line to have arrived at these sites, bringing ice at the glacier mouths to flotation.

Prior to this time, we expect glacier thinning to be coupled to grounding-line retreat farther downstream. Modern analogues of this behavior come from recent observations and numerical modeling, which show that changes at the grounding line of deep marine basins beneath Pine Island and Thwaites Glaciers cause rapid thinning over decadal time scales hundreds of kilometers upstream [*Payne et al.*, 2004; *Favier et al.*, 2014; *Joughin et al.*, 2014]. Further, a model of Holocene retreat of Mackay Glacier located along the Scott Coast (Figure 1c) was used to simulate progressive thinning of the glacier as the grounding line retreated from a location 85 km downstream [*Jones et al.*, 2015]. Model results indicate (i) hundreds of meters of thinning occurs on decadal timescales; (ii) thinning does not significantly lag grounding-line retreat; and (iii) thinning accelerates when grounding-line retreat accelerates over reverse bed slopes [*Jones et al.*, 2015].

The majority of the seafloor over which ice from southern Transantarctic Mountains flowed is concealed beneath the modern Ross Ice Shelf (Figure 1) but is presumed to be covered by deformable glaciomarine sediment [*Alley et al.*, 1989] as found near Ross Island [*Naish et al.*, 2009; *McKay et al.*, 2016] and at a site in the southern Ross Sea [*Webb et al.*, 1979]. Drill cores and seismic reflection profiles collected seaward of the modern ice shelf show that the floor of the central Ross Sea consists of older, more consolidated sediments and localized bedrock outcrops [*Halberstadt et al.*, 2016]. Despite this evidence for a more resistive bed in the north central Ross Sea, ice from Scott and Beardmore Glaciers maintained a low surface slope of $<10^{-3}$ during the LGM, extending more than 1000 km to the grounding line from elevations of ~1000 m at the glacier mouths (Figures 1 and 2). Such gradients, typical of modern ice streams, require either a slippery, low-resistance bed [*Waddington et al.*, 2005; *Parizek and Alley*, 2004] or lightly grounded ice, which would have allowed rapid upstream propagation of changes at the grounding line.

4.2. Grounding-Line Constraints

Scott and Beardmore Glaciers maintained their LGM thicknesses until sometime between ~16.7 and ~14.4 kyr B.P. (Figures 2b and 2d), consistent with ^{14}C dates on foraminifera in marine sediment above till in the northern Ross Sea, near the maximum extent of grounded ice [*Licht*, 2004]. Thereafter, the upper flanks of Mount Rigby and Mount Hope were exposed gradually (Figures 2b and 2d), implying slow grounding-line retreat in the central Ross Sea prior to ~9.3 kyr B.P. Over the next 700 ± 200 years, ice thinned by 200–300 m at both sites, indicating rapid grounding-line incursion into the southern Ross Sea. This episode brought the grounding line close to the mouth of Beardmore Glacier, where ice stood within 80 m of its present level by ~8.6 kyr B.P. Further retreat lowered Beardmore Glacier to its modern level by ~7.8 kyr B.P. and brought the grounding line close to the mouth of Shackleton Glacier by ~7.7 kyr B.P. Scott Glacier, however, remained 400–500 m thicker than present at this time. Rapid thinning at Mount Rigby ~6.3 kyr B.P. (Figure 2b) implies a second episode of rapid grounding-line recession, which was likely limited to the region south of Crary Ice Rise (Figure 1). The inference that this second recession involved only a small portion of the ice sheet is further supported by the fact that ice at lower Reedy Glacier did not thin at this time, in contrast to the rapid retreat that occurred ~9–8 kyr B.P. (Figure 2a). Subsequent thinning at Mount Rigby gradually brought ice to the modern glacier level from ~6.3 to 3.4 kyr B.P. At the end of this period, the Ross Sea grounding line was likely close to its present position between the mouths of Reedy and Scott Glaciers (Figure 1).

4.3. Synchronous Deglaciation of the Central and Western Ross Sea

Arrival of the grounding line at the mouths of Beardmore and Shackleton Glaciers ~9–8 kyr B.P. coincided with final deglaciation of the Scott Coast region, ~800 km north along the Transantarctic Mountains (Figure 1). This indicates that much of the ice in the central and western Ross Sea was evacuated in a single brief period of deglaciation and grounding-line retreat ~9–8 kyr B.P., thereby ruling out the earlier conception of gradual and progressive grounding-line retreat along the Transantarctic Mountains [*Conway et al.*, 1999].

The deglaciation history of the Scott Coast and northern Ross Sea is largely based on radiocarbon ages and is summarized below. Where necessary, published ^{14}C dates have been recalibrated using IntCal13 and Marine13 ^{14}C calibration curves [*Reimer et al.*, 2013] and Southern Ocean marine reservoir corrections [*Hall et al.*, 2010]. We do not rely on ^{14}C measurements on acid-insoluble organic material, as these commonly contain pre-Quaternary carbonaceous material derived from glacial or marine sediment upstream [*Andrews et al.*, 1999]. Apparent ages of acid-insoluble organic matter are therefore often thousands of years older than the depositional age of the sediment. Previously published exposure ages have been recalculated to be consistent with samples presented in this paper.

Relative sea level curves from McMurdo Sound and Terra Nova Bay (Figure 1c) suggest final removal of grounded ice shortly before ~7.8 and ~8.0 kyr B.P., respectively [*Baroni and Hall*, 2004; *Hall et al.*, 2004]. These ages agree with limiting ages from ice-dammed lakes in Taylor Valley [*Hall and Denton*, 2000] and with dates of the oldest postglacial marine shells retrieved from the McMurdo region [*Licht et al.*, 1996; *Kellogg et al.*, 1990]. Exposure ages from near the mouth of Mackay Glacier, which flows across the Scott Coast, indicate rapid thinning to near-modern levels ~7 kyr B.P. [*Jones et al.*, 2015]. Carbon-14 ages of foraminifera in marine sediment recovered ~60 km east of Ross Island indicate open-water conditions there by 8.6 ± 0.25 kyr B.P. [*McKay et al.*, 2016]. This is older than deglaciation ages from farther to the west and may imply that the grounding line retreated shoreward, resulting in open-water conditions at the core site before sites closer to the coast became ice free [*McKay et al.*, 2016; *Lee et al.*, 2017]. Taken together, these ages indicate that grounded ice withdrew from the Scott Coast region between ~8.6 and 7 kyr B.P. Within the uncertainties of the dating methods, this was synchronous with grounding-line retreat past the mouths of Beardmore and Shackleton Glaciers, indicating that grounded ice disappeared from much of the central and western Ross Sea in a period of less than 2 kyr.

4.4. Controls on Rapid Deglaciation ~9–8 kyr B.P.

Rapid deglaciation occurred despite stabilizing conditions of falling relative sea level. By this time, the glacio-isostatic effects of unloading grounded ice around the Ross Embayment exceeded eustatic sea level rise, as shown by relative sea level curves from the Scott Coast [*Baroni and Hall*, 2004; *Hall et al.*, 2004]. The stabilizing effect should have increased southward, because isostatic rebound increased toward the ice sheet interior [*Peltier*, 2004]. Thus, two factors most likely influenced rapid deglaciation in the southern Ross Embayment: (i) enhanced melting at the grounding line and (ii) retreat into deep marine troughs to the south. Although increased ocean heat transport to the marine ice margin may have significantly affected the mass balance,

as presently seen in the Amundsen Sea [*Alley et al.*, 2015], this cannot be verified at present because proxy records of Ross Sea water temperature do not yet exist. Troughs in the western Ross Sea coalesce southward into a deep basin offshore of the Transantarctic Mountains (Figure 1). Because the discharge of marine-based ice sheets increases nonlinearly with ice thickness at the grounding line [*Weertman*, 1974; *Schoof*, 2007], the recession may have accelerated as the grounding line moved into this basin. This applies whether retreat progressed rapidly southward along the mountain front or shoreward from the central Ross Sea (Figure 1). The latter scenario is supported by (i) ^{14}C ages of foraminifera in marine sediment retrieved from ~60 km east of Ross Island [*McKay et al.*, 2016], which predate deglaciation ages from farther west along the Scott Coast (Figure 1c), and (ii) seafloor geomorphic features in the central Ross Sea [*Halberstadt et al.*, 2016] and near Ross Island [*Lee et al.*, 2017], which also indicate shoreward grounding-line retreat.

4.5. Sea Level Contribution

Our results indicate that the Ross Sector's contribution to sea level peaked ~9–8 kyr B.P. Sea level records from sites far from the isostatic influence of ice sheets show large and rapid rises at this time [*Khan et al.*, 2015, and references therein]; however, a large portion of this meltwater likely came from the final stages of Northern Hemisphere deglaciation [*Peltier et al.*, 2015]. Data-constrained ice sheet models indicate that the Ross Sector only contributed 3–4 m to sea level during the entire deglaciation [*Briggs et al.*, 2014; *Whitehouse et al.*, 2012]. We show that much of this meltwater was released 5–6 kyr after MWP-1A, which indicates that the Ross Sector did not significantly contribute to this event. These same models suggest that the total Antarctic sea level contribution during the last deglaciation was ~7–14 m [*Briggs et al.*, 2014; *Whitehouse et al.*, 2012; *Stuhne and Peltier*, 2015; *Golledge et al.*, 2012], less than most estimates of MWP-1A sea level rise [e.g. *Liu et al.*, 2016; *Lambeck et al.*, 2014; *Deschamps et al.*, 2012; *Peltier et al.*, 2015]. Geologic data from around the continent show deglaciation continuing into the late Holocene, long after MWP-1A. None of this evidence is consistent with an Antarctic source for the enormous volume of meltwater released to the oceans in a few hundred years during MWP-1A.

After ~9–8 kyr B.P., the Ross Sector ceased contributing significantly to global sea level rise. As discussed in section 4.2, rapid thinning at Mount Rigby ~6.3 kyr B.P. was likely related to an episode of grounding-line recession that only removed a small portion of the grounded ice in the Ross Sea.

5. Conclusions

We present ice-thinning records from the southern Transantarctic Mountains that constrain the chronology and pattern of grounding-line recession in the Ross Sea. In conjunction with deglaciation constraints from the Scott Coast region, these data reveal an episode of rapid recession in the early Holocene that removed grounded ice from much of the central and western Ross Sea. In contrast, previous reconstructions of Ross Sea deglaciation, based almost exclusively on geologic constraints from the northern Ross Sea, have been forced to infer gradual retreat in the southern Ross Sea [e.g., *Conway et al.*, 1999; *Anderson et al.*, 2014].

During the MWP-1A episode, the Ross Sector neither contributed nor responded significantly to global sea level rise; rather, much of the Ross Sea deglaciated ~9-8 kyr B.P., several thousand years after MWP-1A. Because we can rule out other factors, this episode of rapid retreat was likely influenced by enhanced melting at the grounding line and/or unstable retreat into deep marine basins.

Acknowledgments
Support for this work was provided by U.S. National Science Foundation (NSF) grants 0636818 and 0838818 and the United States Antarctic Program. P.S. received funding from the NSF Graduate Research Fellowship Program. We thank Maurice Conway and Lesley Urasky for assistance in the field, Joy Laydbak and Marcus Gladden for assistance with sample preparation, and Robert Finkel, Dylan Rood, Susan Zimmerman, and Tom Brown for accelerator analyses. Additionally, we thank Andrew Hein, Joanne Johnson, and an anonymous reviewer for constructive feedback. The data described in this paper are included in the supporting information.

References

Ackert Jr., R. P., et al. (2011), West Antarctic Ice Sheet elevations in the Ohio Range: Geologic constraints and ice sheet modeling prior to the last highstand, *Earth Planet. Sci. Lett.*, *307*, 83–93.

Alley, R. B., D. D. Blankenship, S. T. Rooney, and C. R. Bentley (1989), Sedimentation beneath ice shelves—The view from Ice Stream B, *Mar. Geol.*, *85*, 101–120.

Alley, R. B., et al. (2015), Oceanic forcing of ice-sheet retreat: West Antarctica and more, *Ann. Rev. Earth Planet. Sci.*, *43*, 207–231.

Anderson, J. B., et al. (2014), Ross Sea paleo-ice sheet drainage and deglacial history during and since the LGM, *Quat. Sci. Rev.*, *100*, 31–54.

Andrews, J. T., et al. (1999), Problems and possible solutions concerning radiocarbon dating of surface marine sediments, Ross Sea, Antarctica, *Quat. Res.*, *52*, 206–216.

Balco, G., J. O. Stone, N. A. Lifton, and T. J. Dunai (2008), A complete and easily accessible means of calculating surface exposure ages or erosion rates from ^{10}Be and ^{26}Al measurements, *Quat. Geochronol.*, *3*, 174–195.

Baroni, C., and B. L. Hall (2004), A new Holocene relative sea-level curve for Terra Nova Bay, Victoria Land, Antarctica, *J. Quat. Sci.*, *19*, 377–396.

Bindschadler, R. A., E. P. Roberts, and A. Iken (1990), Age of Crary Ice Rise, Antarctica, determined from temperature-depth profiles, *Ann. Glaciol.*, *14*, 13–16.

Borchers, B., et al. (2016), Geological calibration of spallation production rates in the CRONUS-Earth project, *Quat. Geochronol.*, *31*, 188–198.

Briggs, R. D., D. Pollard, and L. Tarasov (2014), A data-constrained large ensemble analysis of Antarctic evolution since the Eemian, *Quat. Sci. Rev.*, *103*, 91–115.
Carlson, A. E., and P. U. Clark (2012), Ice sheet sources of sea level rise and freshwater discharge during the last deglaciation, *Rev. Geophys.*, *50*, 1–72.
Clark, P. U., J. X. Mitrovica, G. A. Milne, and M. E. Tamisiea (2002), Sea-level fingerprinting as a direct test for the source of global meltwater pulse 1A, *Science*, *295*, 2438–2441.
Conway, H., B. Hall, G. Denton, A. Gades, and E. Waddington (1999), Past and future grounding-line retreat of the West Antarctic Ice Sheet, *Science*, *286*, 280–283.
Deschamps, P., et al. (2012), Ice-sheet collapse and sea-level rise at the Bølling warming 14,600 years ago, *Nature.*, *483*, 559–564.
Ditchburn, R. G., and N. E Whitehead (1994), The separation of ^{10}Be from silicates, in *Proceedings of the 3rd Workshop of the South Pacific Environmental Radioactivity Association*, edited by G. Hancock and P. Wallbrink, pp. 4–7, Australian National Univ., Canberra.
Farmer, G. L., K. Licht, R. J. Swope, and J. Andrews (2006), Isotopic constraints on the provenance of fine-grained sediment in LGM tills from the Ross Embayment, Antarctica, *Earth Planet. Sci. Lett.*, *249*, 90–107.
Favier, L., et al. (2014), Retreat of Pine Island Glacier controlled by marine ice-sheet instability, *Nat. Clim. Change*, *4*, 117–121.
Fretwell, P., et al. (2013), Bedmap2: Improved ice bed, surface and thickness datasets for Antarctica, *The Cryosphere*, *7*, 375–393.
Golledge, N. R., et al. (2012), Dynamics of the Last Glacial Maximum Antarctic ice-sheet and its response to ocean forcing, *Proc. Natl. Acad. Sci. U.S.A.*, *109*, 16052–16056.
Halberstadt, A. R. W., et al. (2016), Past ice-sheet behaviour: Retreat scenarios and changing controls in the Ross Sea, Antarctica, *The Cryosphere*, *10*, 1003–1020.
Hall, B. L., C. Baroni, and G. H. Denton (2004), Holocene relative sea-level history of the Southern Victoria Land Coast, Antarctica, *Global Planet. Change.*, *42*, 241–263.
Hall, B. L., and G. H. Denton (2000), Radiocarbon chronology of Ross Sea drift, eastern Taylor Valley, Antarctica: Evidence for a grounded ice sheet in the Ross Sea at the Last Glacial Maximum, *Geogr. Ann. Ser. A Phys. Geogr.*, *82*, 305–336.
Hall, B. L., G. M. Henderson, C. Baroni, and T. B. Kellogg (2010), Constant Holocene Southern-Ocean ^{14}C reservoir age and ice-shelf flow rates, *Earth Planet. Sci. Lett.*, *296*, 115–123.
Jones, R. S., et al. (2015), Rapid Holocene thinning of an East Antarctic outlet glacier driven by marine ice sheet instability, *Nat. Commun.*, *6*, 1–9.
Joughin, I., B. Smith, and B. Medley (2014), Marine ice sheet collapse potentially under way for the Thwaites Glacier Basin, West Antarctica, *Science*, *344*, 735–738.
Jull, A., E. Scott, and P Bierman (2015), The CRONUS-Earth inter-comparison for cosmogenic isotope analysis, *Quat. Geochronol.*, *26*, 3–10.
Kellogg, T., D. Kellogg, and M. Stuiver (1990), Late Quaternary history of the southwestern Ross Sea: Evidence from debris bands on the McMurdo Ice Shelf, Antarctica, *Antarct. Res. Ser.*, *50*, 25–56.
Khan, N. S., et al. (2015), Holocene relative sea-level changes from near-, intermediate-, and far-field locations, *Curr. Clim. Change Rep.*, *1*, 247–262.
Kohl, C., and K. Nishiizumi (1992), Chemical isolation of quartz for measurement of in situ-produced cosmogenic nuclides, *Geochim. Cosmochim. Acta*, *56*, 3586–3587.
Lal, D. (1991), Cosmic-ray labeling of erosion surfaces: In situ nuclide production rates and erosion models, *Earth Planet. Sci. Lett.*, *104*, 424–439.
Lambeck, K., H. Rouby, A. Purcell, Y. Sun, and M. Sambridge (2014), Sea level and global ice volumes from the Last Glacial Maximum to the Holocene, *Proc. of the Nat. Acad. of Sci.*, *111*, 15296–15303.
Lee, J., et al. (2017), *Widespread persistence of expanded East Antarctic glaciers in the southwest Ross Sea during the last deglaciation*, vol. 45, pp. 403–406.
Licht, K. J. (2004), The Ross Sea's contribution to eustatic sea level during meltwater pulse 1A, *Sediment. Geol.*, *165*, 343–353.
Licht, K. J., A. J. Hennessy, and B. M Welke (2014), The U-Pb detrital zircon signature of West Antarctic ice stream tills in the Ross embayment, with implications for Last Glacial Maximum ice flow reconstructions, *Antarct. Sci.*, *26*, 687–697.
Licht, K., A. Jennings, J. Andrews, and K. Williams (1996), Chronology of late Wisconsin ice retreat from the western Ross Sea, Antarctica, *Geology*, *24*, 223–226.
Licht, K. J., J. R. Lederer, and R. J. Swope (2005), Provenance of LGM glacial till (sand fraction) across the Ross embayment, Antarctica, *Quat. Sci. Rev.*, *24*, 1499–1520.
Liu, H., et al. (2001), *Radarsat Antarctic Mapping Project Digital Elevation Model Version*, vol. 2, NSIDC, Boulder, Colo.
Liu, J., G. A. Milne, R. E. Kopp, P. U. Clark, and I. Shennan (2016), Sea-level constraints on the amplitude and source distribution of Meltwater Pulse 1A, *Nature Geosci.*, *9*, 130–134.
Martín, C., R. C. A. Hindmarsh, and F. J. Navarro (2006), Dating ice flow change near the flow divide at Roosevelt Island, Antarctica, by using a thermomechanical model to predict radar stratigraphy, *J. Geophys. Res.*, *111*, F01011, doi:10.1029/2005JF000326.
McKay, R., N. R. Golledge, S. Maas, T. Naish, R. Levy, G Dunbar, and G. Kuhn (2016), Antarctic marine ice-sheet retreat in the Ross Sea during the early Holocene, *Geology*, *44*, 7–10.
Naish, T., et al. (2009), Obliquity-paced Pliocene West Antarctic ice sheet oscillations, *Nature*, *458*, 322–328.
Nishiizumi, K., M. Imamura, M. Caffee, J. R. Souton, R. C. Finkel, and J. McAninch (2007), Absolute calibration of ^{10}Be AMS standards, *Nucl. Instrum. Methods Phys. Res., Sect. B*, *258*, 403–413.
Parizek, B. R., and R. B. Alley (2004), Ice thickness and isostatic imbalances in the Ross Embayment, West Antarctica: Model results, *Global Planet. Change*, *42*, 265–278.
Payne, A. J., A. Vieli, A. P. Shepherd, D. J. Wingham, and E. Rignot (2004), Recent dramatic thinning of largest West Antarctic ice stream triggered by oceans, *Geophys. Res. Lett.*, *31*, L23401, doi:10.1029/2004GL021284.
Peltier, W. R. (2004), Global glacial isostasy and the surface of the ice-age Earth: The ICE-5G (VM2) model and GRACE, *Ann. Rev. Earth Planet. Sci.*, *32*, 111–149.
Peltier, W. R., D. F. Argus, and R. Drummond (2015), Space geodesy constrains ice age terminal deglaciation: The global ICE-6G_C (VM5a) model, *J. Geophys. Res. Solid Earth*, *120*, 450–487, doi:10.1002/2014JB011176.
Reimer, P. J., et al. (2013), IntCal13 and Marine13 radiocarbon age calibration curves 0–50,000 years cal BP, *Radiocarbon*, *55*, 1869–1887.
Rignot, E., J. Mouginot, M. Morlighem, H. Seroussi, and B. Scheuchl (2014), Widespread, rapid grounding line retreat of Pine Island, Thwaites, Smith, and Kohler glaciers, West Antarctica, from 1992 to 2011, *Geophys. Res. Lett.*, *41*, 3502–3509, doi:10.1002/2014GL060140.
Scherer, R. P., et al. (1998), Pleistocene collapse of the West Antarctic Ice Sheet, *Science*, *281*, 82–85.
Schoof, C. (2007), Ice sheet grounding line dynamics: Steady states, stability, and hysteresis, *J. Geophys. Res.*, *112*, F03S28, doi:10.1029/2006JF000664.

Stone, J. O. (2000), Air pressure and cosmogenic isotope production, *J. Geophys. Res.*, *105*, 23,753–23,759.
Stuhne, G. R., and W. R. Peltier (2015), Reconciling the ICE-6G_C reconstruction of glacial chronology with ice sheet dynamics: The cases of Greenland and Antarctica, *J. Geophys. Res. Earth Surf.*, *120*, 1841–1865, doi:10.1002/2015JF003580.
Stuiver, M., G. H. Denton, T. J. Hughes, and J. L. Fastook (1981), History of the marine ice sheets in West Antarctica during the last glaciation: A working hypothesis, in *The Last Great Ice Sheets*, edited by G. H. Denton and T. J. Hughes, pp. 319–439, Wiley-Interscience, New York.
The RAISED Consortium et al. (2014), A community-based geological reconstruction of Antarctic ice sheet deglaciation since the Last Glacial Maximum, *Quat. Sci. Rev.*, *100*, 1–9.
Todd, C., J. Stone, H. Conway, B. Hall, and G. Bromley (2010), Late Quaternary evolution of Reedy Glacier, Antarctica, *Quat. Sci. Rev.*, *29*, 1328–1341.
Waddington, E. D., et al. (2005), Decoding the dipstick: Thickness of Siple Dome, West Antarctica, at the Last Glacial Maximum, *Geology*, *33*, 281–284.
Webb, P. N., T. E. Ronan Jr., J. H. Lipps, and T. E. DeLaca (1979), Miocene glaciomarine sediments from beneath the southern Ross Ice Shelf, Antarctica, *Science*, *203*, 435–437.
Weertman, J. (1974), Stability of the junction of an ice sheet and ice shelf, *J. Glaciol.*, *13*, 3–11.
Whitehouse, P. L., M. J. Bentley, and A. M. Le Brocq (2012), A deglacial model for Antarctica: Geological constraints and glaciological modelling as a basis for a new model of Antarctic glacial isostatic adjustment, *Quat. Sci. Rev.*, *32*, 1–24.

Erratum

In the originally published version of this article, the introduction contained the sentence, "The Antarctic Ice Sheet has been identified as a significant source of Meltwater Pulse 1A (MWP-1A), an abrupt 10-20 m eustatic sea-level rise 14.6 kyr before present (BP) [e.g. *Clark et al*., 2002]." It was corrected to "… Meltwater Pulse 1A (MWP-1A) [e.g. *Clark et al*., 2002], an abrupt ~9-20 m eustatic sea-level rise 14.6 kyr before present (BP) [*Liu et al., 2016; Lambeck et al., 2014; Deschamps et al., 2012; Peltier et al*., 2015]."

In section 4.5, the citation [e.g. *Clark et al*., 2002; *Carlson and Clark*, 2012] was replaced with [e.g. *Liu et al*., 2016; *Lambeck et al*., 2014; *Deschamps et al*., 2012; *Peltier et al*., 2015]. The additional references were added to the Reference section.

These errors have been corrected and this may be considered the official version of record.